

Modeling of the First Layers in the Fly's Eye

J. A. Moya¹, M. J. Wilcox² and G. W. Donohoe¹

Depts. of Electrical and Computer Engineering and Psychology*

NASA ACE Center
 Dept. of Electrical and Computer Engineering
 University of New Mexico, Albuquerque, NM, 87131-1356.
 jamoya@ecece.unm.edu wilcox@cyber.unm.edu donohoe@ecece.unm.edu

Abstract Increased autonomy of robots **would** yield significant advantages in the exploration of space. The shortfalls of computer vision can, however, pose significant limitations on a robot's potential. At the same time, simple insects which are largely hard-wired have effective visual systems. The understanding of insect vision systems thus may lead to improved approaches to visual tasks. A good starting point for the study of a vision system is its eye. In this paper, a model of the sensory portion of the fly's eye is presented. The effectiveness of the model is briefly addressed by a comparison of its performance to experimental data.

1 Introduction

One of the most important sources of information about our environment is certainly vision. Thus, it seems reasonable to endow robots with sight. However, computer vision has proven a difficult problem. At the same time, insects which are essentially hard-wired can solve many visual tasks. These include problems requiring pattern recognition, the tracking of objects and the selection of intercept courses [2,3,10]. Thus, the study of insect vision may lead to new approaches to visual problems.

A most important part of a vision system is its photoreceptor layer. This layer provides the sensory input and therefore sets limits on the performance of the system. Thus, a good starting point for the study of a vision system is in the most distal parts of the eye.

If one wishes to study an insect eye, the eye of the fly is an excellent choice. It is experimentally convenient and much literature on its eye has been produced. In this paper, after an introduction to the fly's eye, a new model of its photoreceptor layer is presented. The effectiveness of the model is also addressed.

2 The distal fly's eye

The eye of the fly is composed of a continuum of layers [1]. The most distal of these are the optical layer, the retina and the **lamina ganglionaris**, usually referred to as simply the **lamina**. The optical layer, the familiar compound structure seen at the eye's surface, is the most visible part of the eye. The term retina as applied to the fly differs from its use in vertebrates, referring only to the portions of photoreceptors distal to their own axons. The **lamina** contains the remaining portions of the photoreceptors and the second-order cells upon which the receptors synapse.

The structure of the fly's distal eye is depicted in fig. 1. The basis element called the **ommatidium** is composed of a pair of optical elements, the **corneal** facet and crystalline cone, and the retinal portions of the photoreceptors that lie immediately under this **dioptric** apparatus [1]. Each eye of a fly contains **several** thousand of these elements. The **ommatidia** are separated from one another by pigment cells which act as apertures and screen out stray light.

The optics are of high quality and deliver a well focused image to the tips of the photoreceptors within the **ommatidium** [6]. Further, because of their **small** size, chromatic aberrations are insignificant and depth of focus is relatively large [6,9].

As depicted in fig. 1B, the photoreceptors contained within the **ommatidium**, are arranged in an asymmetric trapezoid [1], Six peripheral receptors, referred to as **R1** to **R6**, surround a pair of **tandemly** arranged **central** ones, **R7** and **R8**. The central receptors and peripheral receptors are in general of different types and **appear** to serve different functions [5].

The fly's photoreceptor is composed of two parts, the **rhabdomere** and the cell body [1]. The **rhabdomere** acts as an absorbing **waveguide** [19] and transduces light into an ionic current [13]. The cell body can be further divided into three segments, the **soma**, the axon and the axon terminal [1]. The **soma** is the retinal part of the **cell** and receives the current generated in the **rhabdomere**. The terminal is the portion of the cell that transfers information onto second-order cells in the **lamina**. The axon is a conduit that connects the **soma** and terminal.

Unlike many animals with compound eyes, the fly has evolved an "open **rhabdom**" where every **rhabdomere** in the **ommatidium** is optically isolated from its neighbors [1]. In the fly, these **rhabdomeres** also do not collect light

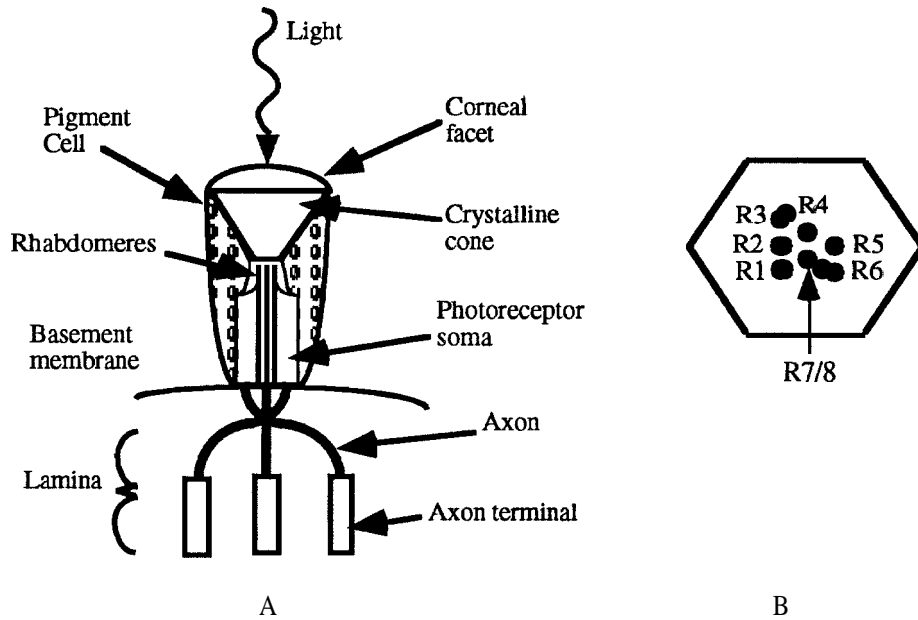


Figure 1 An **ommatidium** in the fly's eye and its **axonal** extensions into the next layer, the **lamina**. **A**. The **ommatidium** is composed of a set of photoreceptors, excluding their axons and axon terminals, and the optics immediately above them, the **corneal** lens and crystalline cone. **Pigment** cells form an aperture around this element and screen out stray light. The **axonal** portions of the receptors synapse with **second-order cells** in the **lamina**. **B**. The **ommatidium** as seen from the top of **A**.

from the same portion of space [8]. Although, as depicted in fig. 2, receptors from six, adjacent **ommatidia** do join together to sample similar regions. These receptors, however, do not sample concentrically [15]. The axons of these same photoreceptors, after penetrating the basement membrane, a high resistance barrier that separates the **extracellular space (ECS)** surrounding the **ommatidia** from the **ECS** of the **lamina**, also join together in the same element in the **lamina** [1].

In these **lamina** structures, new sets of R1 -R6 photoreceptors are grouped. These grouped receptors are referred to as the **neuro-ommatidium**. The axon terminals in a single **neuro-ommatidium** are electrically coupled via gap junctions, allowing light induced currents in one photoreceptor to flow to the other **neuro-ommatidial** receptors [16]. This coupling is restricted to adjacent neighbors (i.e. R1 is coupled to R2 and R6, R2 to R1 and R3, etc.). The central receptors bypass the **neuro-ommatidia**, join the **efferent lamina** axons and continue on to the next **neuropile**, the medulla.

Glial cells perform a similar role to that of the pigment cells in the **ommatidial** layer above, and physically separate the **neuro-ommatidial** axon terminal rings from one another in the **lamina**, creating distinct units called cartridges [17]. This **glial** partitioning **also** results in electrical isolation of the terminal rings [18]. Current does, however, pass through the **glial** cells, effectively coupling these compartments as well. The **neuro-ommatidia**, in like number to the **ommatidia**, are repeated thousands of times across the eye [1].

3 Modeling

The model of a **neuro-ommatidium** can be formulated in two parts, one to account for the **phototransduction** process and the other to account for charge changes in its components. Figure 3 illustrates the nodes and layers required in this model. **Phototransduction** is discussed elsewhere [12].

In the equations presented in this section, the layers in the model concerned with charge changes will be referred to by number, starting with one for references to the membrane current layer. Where a node can be **related** to one of the photoreceptors (i.e. R1 through R6), it is assumed to be designated by the same number as that photoreceptor. When only one node is **present** in a layer, it is designated as node one. The notation used to refer to model quantities will be of two forms. A quantity of the form A_m is a constant. A quantity of the form A_{mnp} refers to a concept associated with processing in the m^{th} node of the n^{th} layer in the p^{th} **neuro-ommatidium**.

Equations to describe intercellular charge changes in R1-R6 photoreceptors and the cartridge **ECS** can be derived from fig. 4 [12]. The resulting equations for the R1-R6 **soma** and terminal are

$$V_2 \dot{X}_{m2p} - B_1 X_{m2p} - B_2 (X_{m2p} - X_{m3p}) + I_{in} \quad (1)$$

$$V_3 \dot{X}_{m3p} - B (X_{m2p} - X_{m3p}) - B_3 (X_{m3p} - X_{i4p}) + B_4 \sum_{i \in C} (X_{i3p} - X_{m3p}) \quad (2)$$

where $C = \{\text{mod}_6(m)+1, \text{mod}_6(m+4)+1\}$.

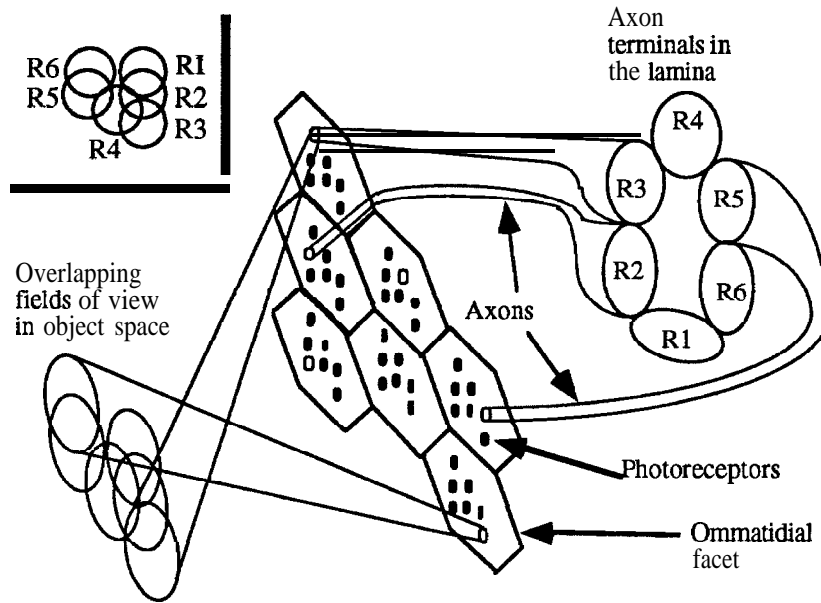


Figure 2 The **neuro-ommatidium** and the sampling pattern of its photoreceptors. The **ommatidial** and **lamina** layers have been flattened. The receptors are depicted as white and black circles within the hexagonal, **ommatidial** facets. Those receptors in white correspond to the depicted **neuro-ommatidium**. The R1-R6 axon terminals of these latter receptors join together to form ring-like structures in the **lamina**. Inset: Every point in space is sampled by six peripheral receptors, each from a different **ommatidium**. A single R1, R2, etc. is used in each of these overlapped samplings.

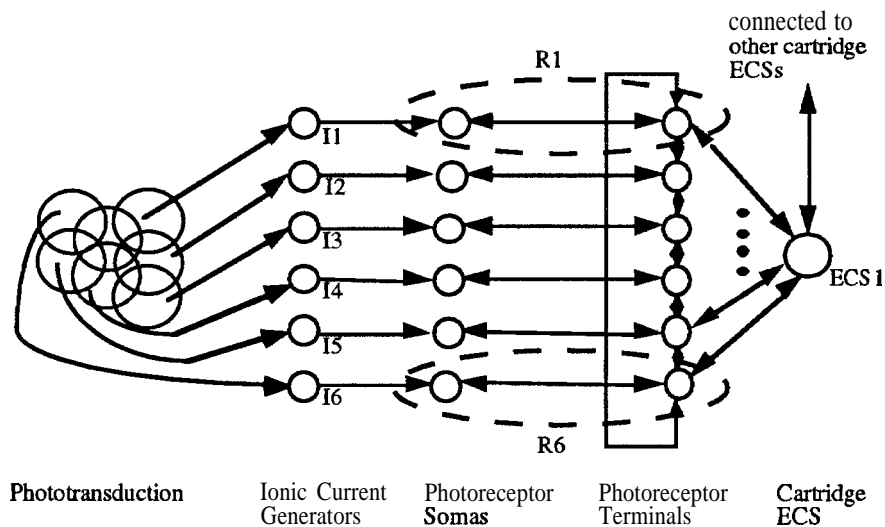


Figure 3 The nodal structure of a model for the flow of charge within the photoreceptors and cartridge ECS of a **neuro-ommatidium**. The arrows are used to indicate the type of coupling that exists between the nodes.

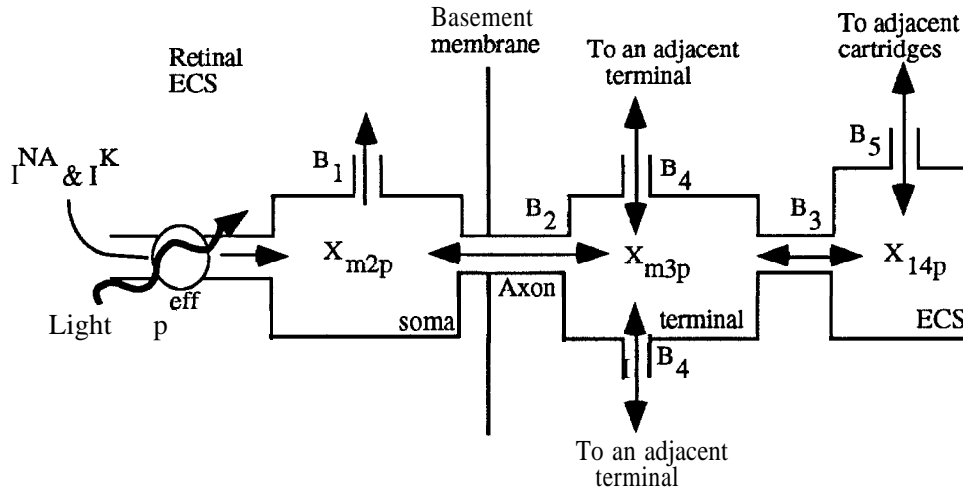


Figure 4 Intercompartmental current flow within an R1-R6 photoreceptor and the cartridge ECS. The arrows are used to indicate the possible directions for charge flow.

The solutions of eqns. 1 and 2 give normalized, lumped, ionic concentrations (NLICs), relative to a lumped ionic concentration in the retinal ECS, for a receptor soma and a receptor axon terminal, respectively. X_{mip} and V_i represent the NLIC and the volume contained within an element in the i^{th} layer. B_r is a coefficient of flow conductance. I_{in} in eqn. 1 is a lumped input current. The set C in eqn. 2 defines the terminals within the cartridge ring that are adjacent to the m^{th} terminal.

The ionic current I_{in} driving the photoreceptor soma should be predominantly composed of Na^+ and K^+ [13,14,20]. These ions are delivered by three different processes [13,20] that can be combined using the equation

$$I_{in} = -I_{m1p}^{\text{Na}} + I_{\text{bkngnd}}^{\text{K}} + I_{m1p}^{\text{K}} \quad (3)$$

I_{m1p}^{Na} is an inward, light-induced, Na^+ current, $I_{\text{bkngnd}}^{\text{K}}$ and I_{m1p}^{K} are also inward currents and are defined as the parts of the K^+ current present in an unstimulated photoreceptor and the current above this background level in a stimulated photoreceptor, respectively. Henceforth, references to a K^+ current should be understood to be concerned with only the latter of these two K^+ currents. Na^+ is typically concentrated on the outside of the cell and K^+ on the inside [14]. The increased flow of each into the cell has a different effect, with increased Na^+ flow reducing the lumped, inside-to-outside concentration difference and K^+ flow raising it. With this in mind, the negation of I_{m1p}^{Na} in eqn. 3 does not reflect a difference in current flow direction, but instead its counter role to that K^+ flow.

Taking the expected membrane current properties into account [12], a set of equations of the form

$$i_{m1p}^{\text{Na}} = -D_1 I_{m1p}^{\text{Na}} + (D_2 \cdot D_3 I_{m1p}^{\text{Na}}) * \Gamma \quad (4)$$

$$i_{m1p}^{\text{K}} = (-I_{m1p}^{\text{K}} + D_4 I_{m1p}^{\text{Na}}) * \Phi \quad (5)$$

can be used to model the Na^+ and K^+ currents, respectively. The D coefficients of eqn. 4 define the saturation and decay properties of the Na^+ current. D_4 in eqn. 5 defines the steady state K^+ to Na^+ ratio. Γ in eqn. 4 is a transfer characteristic between the effective collected light power in the m^{th} photoreceptor of the p^{th} neuro-ommatidium and

the stimulation that induces the opening of the Na^+ channels. This latter characteristic is dependent on the **phototransduction** process of the photoreceptor, which records the illumination level via a **photochemical** reaction [5]. Φ in eqn. 5 is a function that **allows** for the adjustment of the K^+ decay rate with respect to the lighting conditions. The **nature** of Γ and Φ are discussed in [12],

The final equation required for the modeling of the **neuro-ommatidial** photoreceptors and the cartridge ECS is the one **that** describe the charge dynamics of the cartridge ECS itself. This can be **defined** using

$$v_4 \dot{X}_{14p} = B_3 \sum_{i=1}^6 (X_{i3p} - X_{14p}) - B_5 \sum_{j \in S} (X_{14j} - X_{14p}) . \quad (6)$$

The set S in eqn. 6 defines the cartridges that are part of the surround of the p^{th} neuro-ommatidium, i.e. the cartridge neighborhood that due to proximity and the **glial** coupling in the fly's **lamina** significantly affect the ionic concentration within the ECS of the p^{th} cartridge [4,11,18].

Values for the coefficients required in the model were determined using experimental data and a fitting algorithm [12]. The model is capable of reproducing the **responses** seen in a fly for wide-field sinusoidal and step stimulation as well as for single photoreceptor illumination [12]. Figure 5 depicts the sinusoidal response properties of the fly and the model. The differences in the phase response are likely due to system delays that were not taken into account in the model's development. Except for this slight discrepancy, the model behavior is quite representative of that seen in the animal.

4. Conclusions

Animal vision offers the potential for **the** discovery of new approaches to the solution of difficult computer vision problems. The hard-wired nature of insect vision **Wows** the derivation of a model that captures the functionality of an animal's neurons. The equations presented here model the principles used **in** the photoreceptor layer of the fly's eye. This model is capable of reproducing the responses recorded in this animal under various types of stimulation.

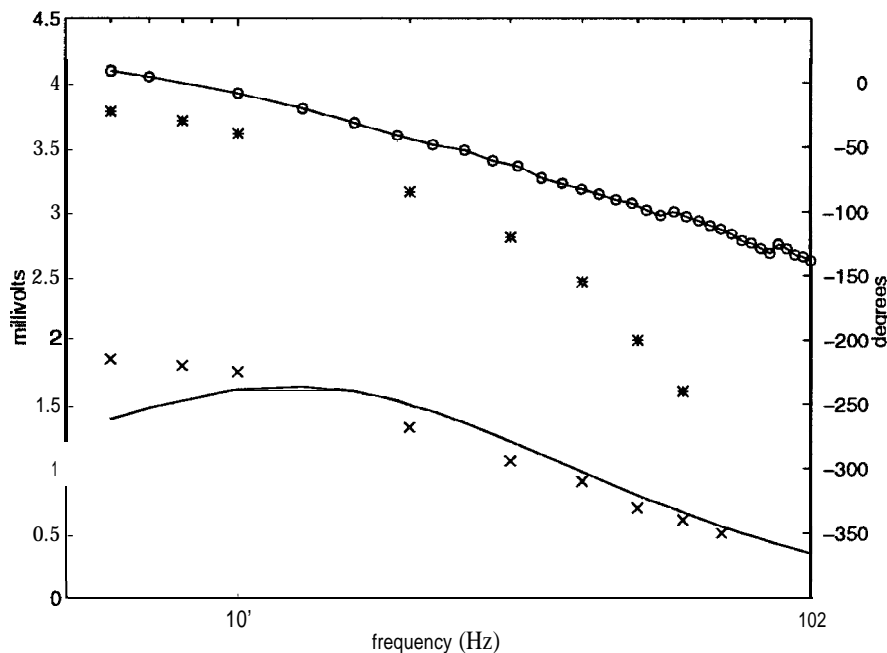


Figure 5 The magnitude and phase of the sinusoidal responses of the model. The details of the stimulation used can be found in [12]. The upper curve (Φ) is the phase response and the lower curve (-) is the magnitude. The data symbolized using “*” and “x” is corresponding experimental results from [7] for fly photoreceptor phase and magnitude responses, respectively. Differences between the model and experimental phase can be attributed to system delays that were not taken into account in the model.

Acknowledgments

This work was performed in the Center for Autonomous Control Engineering at the University of New Mexico. Support was provided in part by NASA under contract NCCW-0087.

References

- [1] **Braitenberg, V.** 1967. **Patterns** of projections in the visual system of the fly. I. **Retina-lamina** projections. *Exp. Brain Res.* 3, 271-298.
- [2] **Collett, T.** and **Land, M.** 1978. How **hoverflies** compute intercept **courses**. *J. Comp. Physiol. A* 125, 191-204.
- [3] **Dill, M., Wolf, R.** and **Heisenberg, M.** 1993. Visual pattern recognition in *Drosophila* involves **retinotopic** matching. *Nature* 365, 751-753.
- [4] **Dubs, A.** 1982. The spatial integration of signals in the retina and **lamina** of the fly compound eye under different conditions of luminance. *J. Comp. Physiol. A* 146, 321-343.
- [5] **Hardie, R.** 1986. The photoreceptor array of the **Dipteran** retina. *TINS* 9,419-423.
- [6] **Horridge, G., Mimura, K.** and **Hardie, R.** 1976. Fly photoreceptors III. Angular sensitivity as a function of wavelength and the limits of resolution. *Proc. R. Soc. Lond. B* 194, 151-177.
- [7] **Järvilehto, M.** and **Zettler, F.** 1971. Localized intracellular potentials **from pre- and postsynaptic** components in the external plexiform layer of an insect retina. *Z. vergl. Physiol.* 75,422-440.
- [8] **Kirschfeld, K.** 1967. Die Projection **der optischen Umwelt** auf **das Raster der Rhabdomere im Komplexauge** von Muses. *Exp. Brain Res.* 3, 248-270.
- [9] **Kuiper, J.** 1966. On the image formation in a single **ommatidium** of the compound eye in **Diptera**. In *The functional organization of the compound eye*, C. G. Bernhard, ed. **Pergamon** Press, New York.
- [10] **Land, M.** and **Collett, T.** 1974. Chasing behavior of houseflies (*Fannia canicularis*): A description and analysis. *J. Comp. Physiol.* 89, 331-357.
- [11] **Mote, M.** 1970. Electrical correlates of neural superposition in the eye of the fly *Sarcophagi bullata*. *J. Exp. Zool.* 175, 159-168.
- [12] **Moya, J.** 1997. Dissertation. (in preparation)
- [13] **Muijser, H.** 1979. The receptor potential of **retinular cells** of the blowfly **Calliphora**: the role of sodium, potassium and calcium ions. *J. Comp. Physiol. A* 132, 87-95.
- [14] **Nicholls, J., Martin, A.** and **Wallace, B.** 1992. *From Neuron to Brain* 3. **Sinauer** Assoc., **Sunderland, MA.**
- [15] **Pick, B.** 1977. Specific misalignments of **rhabdomere** visual axes in the neural superposition eye of **Dipteran** flies. *Biol. Cyber.* 26, 215-224.
- [16] **Ribi, W.** 1978. Gap junctions coupling photoreceptor axons in the first optic ganglion of the fly. *Cell Tiss. Res.* 195, 299-308.
- [17] **Saint Marie, R.** and **Carlson, S.** 1983. **Glial** membrane specializations and the compartmentalization of the **lamina ganglionaris** of the housefly compound eye. *J. Neurocytol.* 12,243-275.
- [18] **Shaw, S.** 1984. Early visual processing in insects. *J. Exp. Biol.* 112, 225-251.
- [19] **Snyder, A.** 1975. Optical properties of invertebrate photoreceptors. In *The compound eye and vision of invertebrates*, G. A. Horridge, ed. **Clarendon** Press, Oxford.
- [20] **Weckström, M., Hardie, R.** and **Laughlin, S.** 1991. Voltage-activated potassium channels in blowfly photoreceptors and their **role** in light adaptation. *J. Physiol.* 440, 635-657.